First-principles study of the magnetization of oxygen-depleted $In_2O_3$(001) surfaces



2009 J. Phys.: Condens. Matter 21 272202

(http://iopscience.iop.org/0953-8984/21/27/272202)

IOP FTC
IOP PUBLISHING JOURNAL OF PHYSICS: CONDENSED MATTER
J. Phys.: Condens. Matter **21** (2009) 272202 (6pp) doi:10.1088/0953-8984/21/27/272202

FAST TRACK COMMUNICATION

# First-principles study of the magnetization of oxygen-depleted $In_2O_3$(001) surfaces

**Z R Xiao, X F Fan, L X Guan, C H A Huan, J L Kuo and L Wang**

Division of Physics and Applied Physics, School of Physical and Mathematical Sciences, Nanyang Technological University, 637371, Singapore

Received 28 April 2009
Published 4 June 2009
Online at stacks.iop.org/JPhysCM/21/272202

**Abstract**
The origin of the magnetism in some oxide-based diluted magnetic semiconductors is still a puzzle. In this work, significantly ferromagnetic states of the oxygen-depleted $In_2O_3$(001) surfaces are investigated on the basis of first-principles density functional calculations. Our results show that the perfect oxygen-depleted surfaces are nonmagnetic; however, the surface states become ferromagnetic with the appearance of vacancies on the most outward In sites. The origin of the surface state magnetization can be explained using the Stoner model, and the exchange coupling between surfaces In s–p hybridization orbitals implies a ferromagnetic ground state. Our investigation gives a reasonable explanation for the source of the magnetism in oxygen-depleted $In_2O_3$ nanostructures observed in previous experiments.

(Some figures in this article are in colour only in the electronic version)

## 1. Introduction

For the last ten years, diluted magnetic semiconductors (DMSs) have received considerable attention as regards both fundamental research and potential applications in spintronics [1, 2]. There are a number of nonmagnetic (NM) metal oxide (MO) matrices, such as ZnO, $TiO_2$, $SnO_2$, and $In_2O_3$, that have been shown to exhibit ferromagnetism with transition metal doping [3–10]. Several undoped MO thin film or nanoparticle systems have been reported to be DMSs [11–13]; however, the origin of the ferromagnetism (FM) for many MO DMSs is still controversial. Theoretical investigations [14–19] have suggested that the intrinsic defects, such as vacancies and interstitials, can also induce spin-polarized states around them inside the MO matrices without any assistance from external transition metal impurities. Such intrinsic defects may contribute some of the magnetic moments in the undoped MO DMS nanostructures; however, the possibility of spin-polarized surface states for such thin films or nanoparticles cannot be ruled out.

Recently, first-principles calculations for the oxides, such as $ZrO_2$, $Al_2O_3$, MgO [20] and ZnO [21], predicted stable magnetic states for the O-terminated surfaces without external magnetic atoms. The origin of the magnetic moments is the spin-polarized 2p holes in the valence band. These results indicate a new path along which to explore the mechanism of the FM in MO DMSs. Nevertheless, the previous theoretical studies only covered the case of magnetization of oxygen-rich surfaces, while many MO DMSs, such as $In_2O_3$ nanostructures, arise only under oxygen-depleted conditions [12, 13]. So far, theoretical investigations [22–24] of the source of the magnetism in the $In_2O_3$ systems mainly focused on extrinsic impurities. Intrinsic defects, e.g. oxygen vacancies, have been stereotyped as assisting the magnetic interactions between those extrinsic impurities. Even though the intrinsic defect model for bulk $In_2O_3$ has been studied [25], there have been no reports on the magnetism induced by intrinsic defects in bulk $In_2O_3$. The studies of the magnetism of the oxides with oxygen-rich surfaces inspire us to consider the possibility that the origin of the magnetic moments of the oxygen-depleted $In_2O_3$ may be the surfaces.

In this work, the electronic structures and magnetic properties of the oxygen-depleted $In_2O_3$ surfaces are studied on the basis of first-principles calculations. Since previous experiments have shown strong magnetic signals of $In_2O_3$ thin film on (001) MgO [12], it is suggested that the magnetization appears on the $In_2O_3$(001) surface. We considered two kinds of perfect oxygen-depleted $In_2O_3$(001) surfaces; however, both structures have no FM ground state. Hence the most possible imperfect surface with two-coordinated surface

 

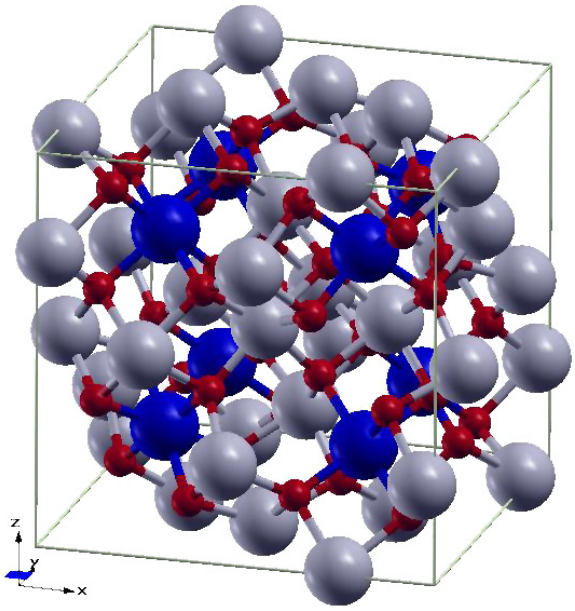


**Figure 1.** The cubic conventional cell of bulk $In_2O_3$. The blue (gray), gray and smaller red (deep gray) spheres represent the $In^1$, $In^2$ and O atoms, respectively.

In vacancies is also explored. Surprisingly, spontaneous magnetization satisfying the Stoner mechanism [26] with FM ordering is found for such defective surfaces. To the best of our knowledge, this is the first theoretical report that s–p hybridized FM states can occur for the intrinsic cations of the oxide surfaces without the assistance of additional magnetic impurities or even oxygen anions. Our discoveries suggest a possible origin of the FM states for the oxygen-depleted $d^0$ oxides: their surface states rather than the oxygen vacancies inside the materials.

## 2. Computational methods

In order to understand the origin of surface magnetization, we investigate the properties of oxygen-depleted $In_2O_3(001)$ surfaces by constructing several representative $In_2O_3$ slabs. We chose a cubic bixbyite-type $In_2O_3$ cell consisting of eight $In^1$ atoms and 24 $In^2$ atoms (figure 1), which correspond to 8b and 24d Wyckoff positions of the $Ia\bar{3}$ group, respectively. The lattice constants $a$ and $b$ of the computational unit cell for the slabs are fixed at 10.309 Å to match the relaxed structure of bulk $In_2O_3$ and slabs are separated by a vacuum of 10 Å. The stacking of the In atoms along the [001] direction is in the form $(4\ In^1 + 4\ In^2)/8\ In^2/(4\ In^1 + 4\ In^2)/8\ In^2$. Therefore, two kinds of perfect oxygen-depleted $In_2O_3(001)$ surfaces corresponding to $In^1 + In^2$-terminated and $In^2$-terminated atomic layers would be expected to appear (figures 2(a) and (b)). Such unit cells consist of 72 In and 96 O atoms. Furthermore, we also consider a most possible defective surface, that is the $In^2$-terminated surface with the most outer atoms ($In^2(2)$) vacant (figure 2(c)), since fewer In–O bondings have to break for forming each vacancy, and such a unit cell includes 68 In and 96 O atoms.

Density functional calculations with the generalized gradient approximation (GGA-PBE) [27] were carried out

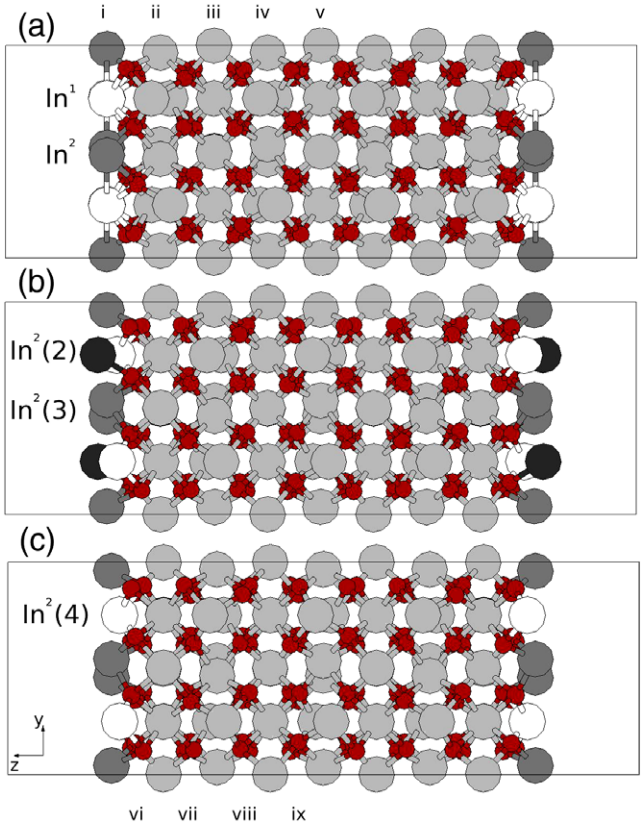


**Figure 2.** The relaxed structures of the slabs for $In_2O_3(001)$: (a) $In^1 + In^2$-terminated surface, (b) $In^2$-terminated surface and (c) the $In^2$-terminated surface with $In^2(2)$ site vacancies. The symbols i–ix indicate the atomic layers of In and O in the $In_2O_3(001)$ slabs. In (a), the white and deep gray spheres represent the surface $In^1$ and $In^2$ atoms. In (b) and (c), the dark, gray and white spheres represent the surface $In^2(2)$, $In^2(3)$ and $In^2(4)$ atoms, respectively. The other light gray and smaller red (deep gray) spheres represent inner In and O atoms.

with the full-potential projector augmented wave (PAW) method [28] implemented in the VASP code [29]. To ensure the accuracy of the electronic calculations, an energy cut-off of 400 eV for the plane wave basis was used and the self-consistent field (SCF) energy convergence criterion was set as $10^{-6}$ eV/atom. For structural relaxations, a conjugate gradient calculation with $3 \times 10^{-2}$ eV $Å^{-1}$ force convergence criterion was applied to the fixed computational unit cell, and a $3 \times 3 \times 1$ $k$-point grid was used to sample the Brillouin zone. To obtain the DOS spectrum, a finer $4 \times 4 \times 1$ $k$-point grid was used.

## 3. Results and discussion

For the $In_2O_3$ bulk system, the coordination numbers (CNs) of the In and O are 6 and 4, respectively. However, the CN of an atom on an $In_2O_3$ surface is altered due to the breaking of the In–O bonding. The CNs of In atoms on (001) surfaces are varied from 2 to 4, depending upon the positions along the $c$-axis. For the oxygen-depleted $In^1 + In^2$-terminated surfaces (figure 2(a)), the differences in height between $In^1$ and $In^2$ atoms are less than $10^{-3}$ Å, and the CNs of $In^1$ and

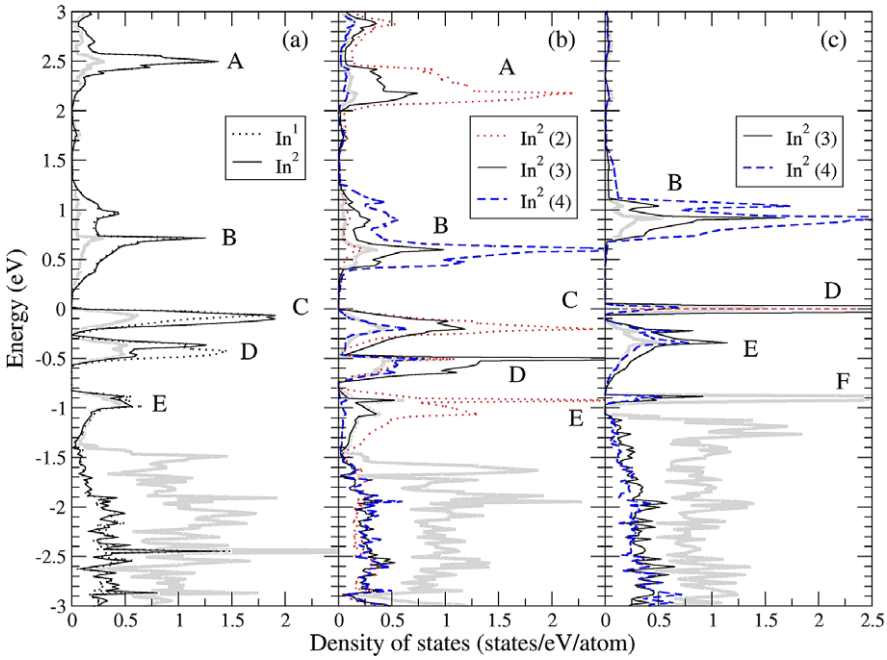


**Figure 3.** The partial density of states (PDOS) of nonmagnetic (NM) $In_2O_3(001)$ surface states on (a) the $In^1 + In^2$-terminated surface, (b) the $In^2$-terminated surface and (c) the $In^2$-terminated surface with $In^2(2)$ site vacancies. The thick gray solid lines represents the surface oxygen (layer (vi) in figure 2) signals. The characters A–F indicate the peaks of surface states.

$In^2$ are both 3. On the other hand, there are three kinds of $In^2$ atoms with various heights on the $In^2$-terminated surfaces (figure 2(b)). The CNs of surface $In^2(2)$, $In^2(3)$ and $In^2(4)$ atoms are 2, 3 and 4, respectively. The changes of the CN of the surface In atoms affect the electronic structures of the surface layers. On the basis of the ionic model, the valence of the indium in the bulk system is 3+, and there is no extra valence electron on an In site. However, the CNs of the surface In atoms drop to 2, 3 or 4, and the corresponding nonbonding electrons for each site are 2, 1.5 and 1, respectively. For the unit cell of $In^1 + In^2$-terminated surfaces, there are four $In^1$ and four $In^2$ atoms on each side of the surface, and they contribute twelve nonbonding electrons for each unit surface. Similarly, there are two $In^2(2)$, four $In^2(3)$ and two $In^2(4)$ atoms for each side of the $In^2$-terminated surface per unit cell, and they also provide twelve nonbonding electrons. If the $In^2(2)$ atoms are removed, the number of nonbonding electrons decreases to 8. The dangling bonds contributed by surface atoms are expected to form surface states, while some of them are occupied by nonbonding electrons.

### *3.1. The nonmagnetic electronic structures of $In_2O_3(001)$ surfaces*

First, we discuss the perfect oxygen-depleted $In_2O_3(001)$ surfaces including the $In^1 + In^2$-terminated and $In^2$-terminated cases. Figure 3 shows the nonmagnetic (NM) density of states (DOS) for the surface In and O. We found the signals of the DOS near the Fermi level which are dominated by surface layers and not observed for bulk $In_2O_3$, so this implies that these states can be classified as surface states. For the perfect oxygen-depleted $In_2O_3(001)$ surfaces without surface In vacancies, five surface states dominated by In s–p hybridization orbitals can be observed (figures 3(a) and (b)). The d orbitals of the In are still fully occupied in the valence bands even for the surface atoms; therefore the d orbitals have little effect on the surface states. On each side of the surface in the unit cell, surface states C, D and E are individually occupied by four extra valence electrons. Even though the total DOS spectra for the two kinds of perfect surfaces are quite similar, there are some different features which can be worked out from the partial DOS (PDOS). It is clear that the PDOS spectra of the $In^1$ and $In^2$ sites are very similar to each other for the $In^1 + In^2$-terminated surface. In contrast, the deviations of PDOS signals are obvious between $In^2(2)$, $In^2(3)$ and $In^2(4)$ sites on the $In^2$-terminated surface, since the states B, D and the other surface states on the $In^2$-terminated surface are dominated by $In^2(4)$, $In^2(3)$ and $In^2(2)$ sites, respectively. These results suggest that the site-dependent occupations of the surface states are induced by the variation of the coordination numbers or the valence charges among surface atoms. We also observed that the energy of the surface state D on the $In^2$-terminated surface is about 0.2 eV lower than that on the same state on the $In^1 + In^2$-terminated surface. This means that the $In^2$-terminated surface might be more stable than the $In^1 + In^2$-terminated surface. The calculation results also indicate that the total energy of the $In^2$-terminated surface is 115 meV lower than that of the $In^1 + In^2$-terminated surface for each side of the surface in a unit cell.

Now we consider the electronic structures of the $In^2$-terminated surfaces with $In^2(2)$ vacancies. When the $In^2(2)$ atoms are removed, the surface electronic structures shown in figure 3(c) exhibit that the states A and C are eliminated. Nevertheless, the surface states F coming from the $In^2(2)$–O

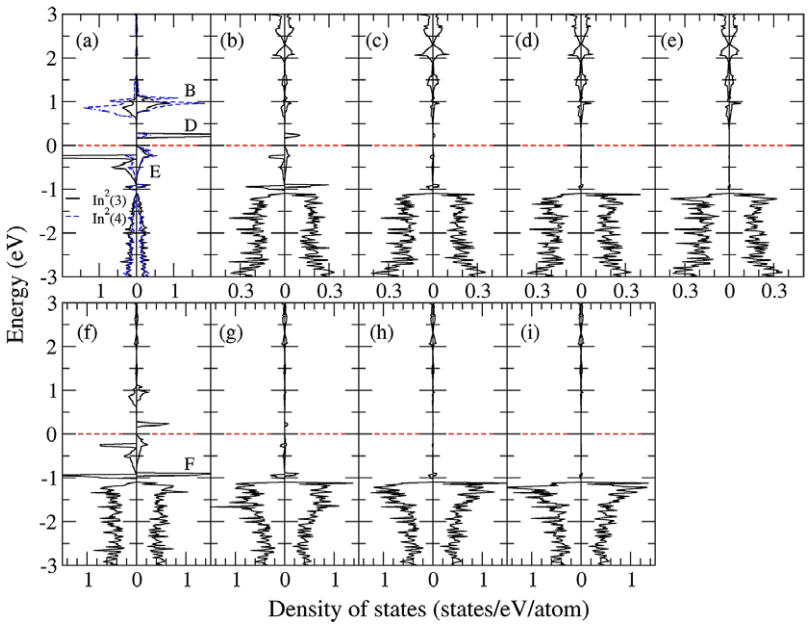


**Figure 4.** The layer-decomposed DOS of the magnetic $In_2O_3(001)$ $In^2$-terminated surface with $In^2(2)$ site vacancies. The spectra in (a)–(e) and (f)–(i) correspond to the DOS signals of In layers (i)–(v) and O layers (vi)–(ix) in figure 2(c), respectively. For each figure, the left and right parts relate to spin majority and minority states, respectively.

broken bonds are formed, consequently. For each side of the surface in the unit cell, the state F receives two nonbonding electrons fed by surface indium atoms. Therefore, the $In^2(3)$-dominated state D becomes half-occupied under the NM condition, which has the possibility of inducing spontaneous magnetization.

### *3.2. The magnetic electronic structures of $In_2O_3(001)$ surfaces*

In order to investigate the magnetic properties of the $In_2O_3(001)$ surface, we performed spin-polarized density functional calculations. Our results show that the electronic structures for perfect $In^1 + In^2$-terminated and $In^2$-terminated surfaces still converge to NM states. In contrast, the stable ferromagnetic (FM) state was found for the $In^2$-terminated surface with $In^2(2)$ vacancies. The layer-decomposed DOS spectra are depicted in figure 4. We observed asymmetry of signals between majority and minority states near the surface layers, especially the In layers (i), (ii) and O layer (vi), which indicates that the magnetization occurs for the surface states. The exchange splits of the surface states D and E are about 0.4 eV and 0.3 eV, respectively. Such splits cause electron transfer from the minority D state to majority D state; therefore, this implies the appearance of magnetic moments of 2 $\mu_B$ for each side of the surface per unit cell, where the average magnetic moments on the $In^2(3)$, $In^2(4)$ and surface oxygen atoms are 0.27 $\mu_B$, $-0.08$ $\mu_B$ and 0.03–0.05 $\mu_B$, respectively. The magnetization energy, defined as the energy difference between the NM and the magnetic states for each side of the surface per unit cell, is found to be 205 meV. This shows that the FM state is more stable than the NM state for the $In^2$-terminated surface with $In^2(2)$ vacancies.

If the previous observations of the magnetic moments on the $In_2O_3$ thin films [12] only come from the surfaces, the density of the surface moments for thin films and nanoparticles is $4.8 \times 10^{-5}$ emu cm$^{-2}$. Our result is 2 $\mu_B$ for each side of the surface per unit cell, or $1.74 \times 10^{-6}$ emu cm$^{-2}$. The apparent deviations of the surface magnetic moment density between the experimental values and our theoretical value may reflect the uncertainties of the assumptions for the effective surface area, e.g. the effective surface area for the thin films would increase due to the surface roughness. Nevertheless, our calculations still confirm that the magnetic moments of the surface states on oxygen-depleted $In_2O_3$ nanostructures must be an important source of overall magnetization, since the order of magnitude of the calculated surface moments does not depart too far from the observed moments.

The origin of the magnetization is the exchange interactions on the $In^2(3)$-dominated surface state D. The bandwidth of such a state is only about 0.1 eV as shown in figures 3(c) and 4(a), which implies that the peak of the PDOS for surface state D is larger than 5 states eV$^{-1}$ for the $In^2(3)$ atoms. It is known that the exchange–correlation integral $I$ for In atoms is about 0.4 eV [26]. According to the Stoner criterion [26], spontaneous magnetization can occur on surface state D. For the FM condition, the exchange coupling between $In^2(3)$ and $In^2(4)$ through sharing oxygen is anti-parallel, because the source of the magnetic moments on the $In^2(4)$ site is the increase in minority state E under magnetization.

We also considered possible antiferromagnetic (AFM) configurations of oxygen-depleted $In_2O_3(001)$ $In^2$-terminated surfaces with $In^2(2)$ vacancies to study the stability of the FM surface state and the exchange interactions among the surface atoms. The spin density distributions of A-, B-, C-type AFM and FM surface states are shown in figure 5. The A-type and B-type AFM configurations are different, because all of the $In^2(3)$ sites at the surface are aligned with $x = 0.25 \pm 0.005$,

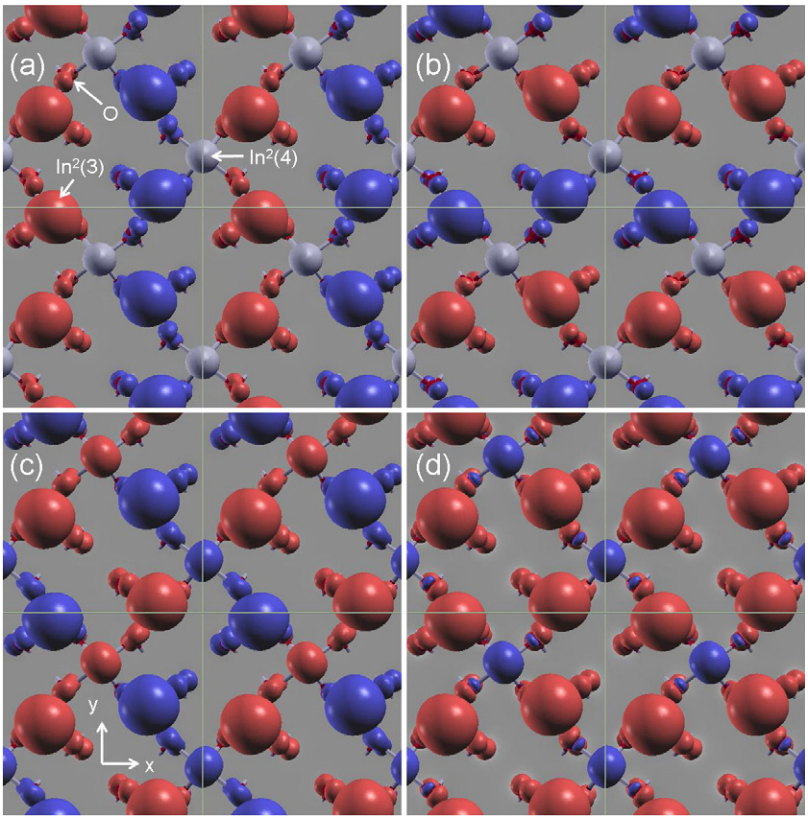


**Figure 5.** The (a) A-type, (b) B-type, (c) C-type AFM and (d) FM configurations of the $In_2O_3(001)$ $In^2$-terminated surface with $In^2(2)$ site vacancies. The red (brighter) and blue (darker) surfaces indicate the isovalues of the spin density (majority–minority) of 0.01 $\mu_B$ $Å^{-3}$ and $-0.01$ $\mu_B$ $Å^{-3}$, respectively. The green (light gray) lines are the unit cell boundaries.

$0.75\pm0.005$ and $y = 0.0\pm0.0433, 0.5\pm0.0433$ after structural relaxation. Therefore, the A-type AFM cannot transform into B-type AFM under symmetry operations. The magnetization energies for A-, B-, and C-type AFM states are 50 meV, 44 meV, and 143 meV, respectively. This implies that the FM state is the most stable magnetization state, while the C-type AFM state is the most stable AFM state. We observed that the absolute values of magnetic moments on $In^2(4)$ atoms for A- and B-type AFM states are 0.00 $\mu_B$, while they are 0.08 $\mu_B$ for the C-type AFM and FM cases. For A- and B-type AFM states, the elimination of the magnetic moments on the $In^2(4)$ sites is due to the preservation of the $c_2$ rotational operation on the $In^2(4)$ sites, while the nonzero magnetic moments on the $In^2(4)$ sites for C-type AFM and FM cases still obey such symmetry operations. The elimination of the magnetic moments on the $In^2(4)$ sites blocks the actions of the exchange splitting; therefore the total energies for A- and B-type AFM states are rising. As regards the FM and C-type AFM cases, the increasing of the energy for the C-type AFM state comes from the existence of parallel coupling between $In^2(3)$ and $In^2(4)$ sites, which interrupts the natural exchange coupling between $In^2(3)$ and $In^2(4)$.

## 4. Conclusions

In conclusion, here, the magnetic states of the oxygen-depleted $In_2O_3(001)$ surfaces have been investigated on the basis of first-principles density functional calculations. Spontaneous magnetization can occur on the $In^2$-terminated surface with $In^2(2)$ site vacancies, while they are still nonmagnetic (NM) for the perfect $In^1$-terminated and $In^2$-terminated surfaces. The origin of the spontaneous magnetization on the surfaces is the half-filling of the surface states consisting of the In s–p hybridization orbitals, and the magnetization mechanism can be explained using the Stoner model. The FM state is the most stable magnetic phase, as is found by comparing the magnetization energies with those of the other A-, B- and C-type AFM states, since these AFM states interfere with the natural exchange coupling between $In^2(3)$ and $In^2(4)$ through sharing oxygen. Unlike previous models, e.g. oxygen-rich oxide surfaces or vacancies inside the oxides, our research demonstrates robust FM states of a novel type, induced by the defective oxygen-depleted oxide surfaces, and it gives a new direction for clarifying the controversial derivations of the magnetism in oxygen-depleted $d^0$ oxides.

## Acknowledgments

This work was supported by the Singapore A*star SERC grant No. 062 101 0030 and the Ministry of Education of Singapore under Grants RG34/05, RG57/05, RG59/06, RG53/08 and T207B1217.

## References

[1] Ohno H 1998 *Science* **281** 951
[2] Prinz G A 1998 *Science* **282** 1660
[3] Venkatesan V, Fitzgerald C B, Lunney J G and Coey J M D 2004 *Phys. Rev. Lett.* **93** 177206
[4] Sluiter M H F, Kawazoe Y, Sharma P, Inoue A, Raju A R, Rout C and Waghmare U V 2005 *Phys. Rev. Lett.* **94** 187204
[5] Neal J R, Behan A J, Ibrahim R M, Blythe H J, Ziese M, Fox A M and Gehring G A 2006 *Phys. Rev. Lett.* **96** 197208
[6] Wang Z and Tang J 2003 *J. Appl. Phys.* **93** 7870
[7] Griffin K A, Pakhomov A B, Wang C M, Heald S M and Krishnan K M 2005 *Phys. Rev. Lett.* **94** 157204
[8] Ogale S B, Choudhary R J, Buban J P, Lofland S E, Shinde S R, Kale S N, Kulkarni V N, Higgins J, Lanci C, Simpson J R, Browning N D, Das Sarma S, Drew H D, Greene R L and Venkatesan T 2003 *Phys. Rev. Lett.* **91** 077205
[9] Coey J M D, Douvalis A P, Fitzgerald C B and Venkatesan M 2004 *Appl. Phys. Lett.* **84** 1332
[10] Philip J, Punnoose A, Kim B I, Reddy K M, Layne S, Holmes J O, Satpati B, LeClair P R, Santos T S and Moodera J S 2006 *Nat. Mater.* **5** 298
[11] Venkatesan M, Fitzgerald C and Coey J M D 2004 *Nature* **430** 630
[12] Hong N H, Sakai J, Poirot N and Brize V 2006 *Phys. Rev.* B **73** 132404
[13] Sundaresan A, Bhargavi R, Rangarajan N, Siddesh U and Rao C N R 2006 *Phys. Rev.* B **74** 161306(R)
[14] Das Pemmaraju C and Sanvito S 2005 *Phys. Rev. Lett.* **94** 217205
[15] Osorio-Guillen J, Lany S, Barabash S V and Zunger A 2006 *Phys. Rev. Lett.* **96** 107203
[16] Bouzerar G and Ziman T 2006 *Phys. Rev. Lett.* **96** 207602
[17] Zuo X, Yoon S-D, Yang A, Vittoria C and Harris V G 2008 *J. Appl. Phys.* **103** 07B911
[18] Xiao Z R, Guo G Y, Lee P H, Hsu H S and Huang J C A 2008 *J. Phys. Soc. Japan* **77** 023706
[19] Zuo X, Yoon S-D, Yang A, Duan W-H, Vittoria C and Harris V G 2009 *J. Appl. Phys.* **105** 07C508
[20] Gallego S, Beltrán J I, Cerdá J and Muñoz M C 2005 *J. Phys.: Condens. Matter* **17** L451
[21] Sanchez N, Gallego S and Munoz M C 2008 *Phys. Rev. Lett.* **101** 067206
[22] Gupta A, Cao H, Parekh K, Rao K V, Raju A R and Waghmare U V 2007 *J. Appl. Phys.* **101** 09N513
[23] Hu S, Yan S, Lin X, Yao X, Chen Y, Liu G and Mei L 2007 *Appl. Phys. Lett.* **91** 262514
[24] Raebiger H, Lany S and Zunger A 2008 *Phys. Rev. Lett.* **101** 027203
[25] Lany S and Zunger A 2007 *Phys. Rev. Lett.* **98** 045501
[26] Janak J F 1977 *Phys. Rev.* B **16** 255
[27] Perdew J P, Burke K and Ernzerhof M 1996 *Phys. Rev. Lett.* **77** 3865
[28] Blöchl P E 1994 *Phys. Rev.* B **50** 17953
[29] Kresse G and Hafner J 1993 *Phys. Rev.* B **48** 13115
Kresse G and Furthmüller J 1996 *Comput. Mater. Sci.* **6** 15
Kresse G and Furthmüller J 1996 *Phys. Rev.* B **54** 11169